

2393-313.04-79711

**NBSIR 75-781**

# **Optical Materials Characterization**

---

Albert Feldman, Deane Horowitz, and Roy M. Waxler

Inorganic Materials Division  
Institute for Materials Research

and

Irving H. Malitson and Marilyn J. Dodge

Optical Physics Division  
Institute for Basic Standards  
National Bureau of Standards  
Washington, D. C. 20234

August 1975

Semi-Annual Technical Report  
Period Covered: January 1, 1975 to July 31, 1975

ARPA Order No. 2620

Prepared for  
**Advanced Research Projects Agency**  
**Arlington, Virginia 22209**



NBSIR 75-781

## OPTICAL MATERIALS CHARACTERIZATION

Albert Feldman, Deane Horowitz, and Roy M. Waxler

Inorganic Materials Division  
Institute for Materials Research

and

Irving H. Malitson and Marilyn J. Dodge

Optical Physics Division  
Institute for Basic Standards  
National Bureau of Standards  
Washington, D. C. 20234

August 1975

Semi-Annual Technical Report  
Period Covered: January 1, 1975, to July 31, 1975  
ARPA Order No. 2620

Prepared for  
Advanced Research Projects Agency  
Arlington, Virginia 22209



---

**U.S. DEPARTMENT OF COMMERCE, Rogers C.B. Morton, *Secretary***  
**James A. Baker, III, *Under Secretary***  
**Dr. Betsy Ancker-Johnson, *Assistant Secretary for Science and Technology***  
**NATIONAL BUREAU OF STANDARDS, Ernest Ambler, *Acting Director***







## OPTICAL MATERIALS CHARACTERIZATION

### Abstract

The refractive index of each of two prismatic samples of chemical vapor deposited (CVD) ZnSe was measured from 0.5086  $\mu\text{m}$  to 18.2  $\mu\text{m}$  by means of the minimum-deviation method on a precision spectrometer. Data were obtained at temperatures near 20 °C and 34 °C and each set of data was fitted to a three-term Sellmeier-type dispersion equation, which permits refractive index interpolation within several parts in  $10^{-5}$ . From the data obtained at the two temperatures,  $dn/dT$  was calculated for both samples. A comparison of refractive index and  $dn/dT$  is made with other types of ZnSe. Preliminary photoelastic data are presented for single crystal specimens of Ge, reactive atmosphere processed (RAP) KCl, and KCl doped with KI. The Ge data, which was obtained at 10.6  $\mu\text{m}$ , differs from previously reported data. Data on the two types of KCl were obtained at 10.6  $\mu\text{m}$ , 0.633  $\mu\text{m}$  and 0.644  $\mu\text{m}$ . These data are compared with values from the literature. Also presented are revised photoelasticity data for CVD ZnSe. The design of an improved stressing apparatus that was developed for the measurement of photoelastic constants is discussed.



## Table of Contents

1. Technical Report Summary . . . . .	1
1.1 Technical Problem. . . . .	1
1.2 General Methodology. . . . .	1
1.3 Technical Results. . . . .	1
1.4 Department of Defense Implications . . . . .	2
1.5 Implications for Further Research. . . . .	2
2. Technical Report	
2.1 Refractive Index and Temperature Coefficient of Index of CVD Zinc Selenide - Marilyn J. Dodge and Irving H. Malitson. . . . .	3
2.1.1 Introduction . . . . .	3
2.1.2 Experimental Technique . . . . .	3
2.1.3 Index Data . . . . .	5
2.1.4 Temperature Coefficient of Index . . . . .	7
2.1.5 Conclusions. . . . .	7
2.2 Photoelastic Constants of Infrared Materials - Albert Feldman, Deane Horowitz and Roy M. Waxler . . . . .	8
2.2.1 Introduction . . . . .	8
2.2.2 The Stress-Optical Constants . . . . .	8
2.2.3 Stress-Induced Birefringence . . . . .	8
2.2.4 Absolute Change of Refractive Index. . . . .	9
2.2.5 Results. . . . .	12
2.2.6 References . . . . .	12

2.3 Revised Photoelastic Data for CVD ZnSe . . . . .	14
2.3.1 References . . . . .	15
2.4 An Improved Apparatus for Photoelasticity Measurements - Albert Feldman and William J. McKean . . . . .	16
2.4.1 References . . . . .	16
3. Acknowledgements . . . . .	18

## OPTICAL MATERIALS CHARACTERIZATION

### 1. Technical Report Summary

#### 1.1 Technical Problem

Windows subjected to high-average-power laser radiation will undergo optical and mechanical distortion due to absorption heating. If the distortion becomes sufficiently severe, the windows become unusable. Theoretical calculations of optical distortion in laser windows depend on the following material parameters: absorption coefficient, refractive index, change of index with temperature, thermal expansion coefficient, stress-optical constants, elastic compliances, specific heat, thermal conductivity and density. Our program has been established to measure refractive indices, changes of index with temperature, stress-optical constants, elastic compliances, and thermal expansion coefficients of candidate infrared laser window materials.

#### 1.2 General Methodology

Laboratory experiments are conducted for measuring refractive indices, changes of index with temperature, stress-optical constants, elastic compliances, and thermal expansion coefficients.

The refractive indices of prismatic specimens are measured on precision spectrometers by using the method of minimum deviation. Two spectrometers are used. One instrument, which uses glass optics, is used for measuring refractive indices in the visible with an accuracy of several parts in  $10^6$ . The other instrument, which uses mirror optics, is used for measuring refractive indices in the ultraviolet and the infrared to an accuracy of several parts in  $10^5$ . Using both spectrometers we can measure refractive indices over the spectral region  $0.2 \mu\text{m}$  to  $50 \mu\text{m}$ .

We measure the coefficient of linear thermal expansion,  $\alpha$ , by a method of Fizeau interferometry. The interferometer consists of a specially prepared specimen which separates two flat plates. Interference fringes are observed due to reflections from the plate surfaces in contact with the specimen. We obtain  $\alpha$  by measuring the shift of these interference fringes as a function of temperature.

The change of refractive index with temperature,  $dn/dT$ , is measured by two methods. In the first method, we measure the refractive index with the precision spectrometers at two temperatures,  $20^\circ\text{C}$  and  $30^\circ\text{C}$ , by varying the temperature of the laboratory. This provides us with a measure of  $dn/dT$  at room temperature. The second method may be used for measuring  $dn/dT$  up to a temperature of  $800^\circ\text{C}$ . We obtain  $dn/dT$  from a knowledge of the expansion coefficient and by measuring the shift of Fizeau fringes in a heated specimen as a function of temperature. The Fizeau fringes are due to interferences between reflections from the front and back surfaces of the specimens.

We measure stress-optical coefficients and elastic compliances using a combination of Twyman-Green and Fizeau interferometers. From the shift of fringes in specimens subjected to uniaxial or hydrostatic compression, we obtain the necessary data for determining all the stress-optical constants and elastic compliances. In materials with small stress-optical constants or in materials that cannot withstand large stress, we measure the stress-optical effect with a modified Twyman-Green interferometer, which has a sensitivity of about  $0.01\lambda$  at  $10.6 \mu\text{m}$ . In this case we must know the elastic constants of the material in order to calculate the stress-optical constants.

#### 1.3 Technical Results

The refractive index of each of two prismatic samples of chemical vapor deposited (CVD) ZnSe was measured from  $0.5086$  to  $18.2 \mu\text{m}$  by means of the minimum-deviation method on a precision spectrometer. Data were obtained at temperatures near  $20^\circ\text{C}$  and  $34^\circ\text{C}$  and each set of data was fitted to a three-term Sellmeier-type dispersion equation, which permits refractive index interpolation within several parts in  $10^{-5}$ . From the data obtained at the two temperatures,  $dn/dT$  was calculated for both samples. A comparison of refractive index and  $dn/dT$  is made with other types of ZnSe. (Section 2.1).

Preliminary photoelastic data are presented for single crystal specimens of Ge, reactive atmosphere processed (RAP) KCl, and KCl doped with KI. The Ge data, which was obtained at  $10.6 \mu\text{m}$ , differ from previously reported data. Data on the two types of KCl were obtained at  $10.6 \mu\text{m}$ ,  $0.633 \mu\text{m}$ , and  $0.644 \mu\text{m}$ . These data are compared with values from the literature. (Section 2.2).

Also presented are revised photoelasticity data for CVD ZnSe (Section 2.3).

In section 2.4 we discuss the design of an improved stressing apparatus that we have developed and are using in our photoelasticity measurements.

#### 1.4 Department of Defense Implications

The Department of Defense is currently constructing high-power infrared laser systems. Criteria are needed for determining the suitability of different materials for use as windows in these systems. The measurements we are performing provide data that laser system designers can use for determining the optical performance of candidate window materials.

#### 1.5 Implications for Further Research

Measurements of refractive index, change of index with temperature, thermal expansion, stress-optical coefficients, and elastic compliances will be continued on candidate laser window materials. More specifically, we plan to complete measurements on the RAP KCl and KCl doped with KI in the infrared at 10.6  $\mu\text{m}$  and in the visible.

We plan to assemble equipment for measuring photoelastic constants at the HeNe wavelength of 3.39  $\mu\text{m}$ . These measurements are of interest to designers of chemical laser systems that operate in the 3-5  $\mu\text{m}$  range. We plan to measure the photoelastic constants of the specimens we have previously measured at other wavelengths (CVD ZnSe, RAP KCl, KCl doped with KI, Ge, chalcogenide glass and As<sub>2</sub>S<sub>3</sub> glass). Furthermore, we are preparing single crystal specimens of LiF and NaF that we will be sending to a commercial firm for polishing.

## 2. TECHNICAL REPORT

### 2.1 Refractive Index and Temperature Coefficient of Index of CVD Zinc Selenide

Marilyn J. Dodge and Irving H. Malitson

#### 2.1.1 Introduction

The performance of a high-power laser system could be limited because of optical distortion of the window material. It has been reported [1] that the effect of a heated window can distort the beam and thus degrade the system at powers less than those required to fracture or melt the window. To predict the amount of distortion which can occur, it is necessary to know the refractive index,  $n$ , temperature coefficient of index,  $dn/dT$ , and the thermal-expansion and stress-optical coefficients of the material under consideration. An optical materials characterization program [2] is currently in progress at NBS to determine these pertinent optical properties. Although much work has been done to predict theoretically the  $dn/dT$  of candidate laser window materials, there is a lack of experimental data on refractive index and  $dn/dT$  to back up the theoretical calculations [3]. The refractometry laboratory at NBS is determining the index of refraction and  $dn/dT$  of selected window materials over a limited temperature range.

Chemical vapor deposited (CVD) zinc selenide is an important candidate window material. This polycrystalline material has a practical transmission range from 0.5 to 20.0  $\mu\text{m}$ . A literature search has revealed that a comprehensive study of the refractive index and  $dn/dT$  of this material over its entire useful transmission range has not been reported. In addition to predicting distortion effects, this data is needed for designing lenses, prisms, and other transmitting components for use in laser systems operating in the 2 - 14  $\mu\text{m}$  range. This paper will present a study on the refractive index and  $dn/dT$  for two samples of CVD ZnSe. Both samples were made by Raytheon Company and are arbitrarily designated as sample A and sample B. Sample A was manufactured about 1971 and sample B in 1974. Sample B appeared to be optically better material than sample A and is considered by the manufacturer to be representative of what is now commercially available.

#### 2.1.2 Experimental Technique

Both specimens were in prismatic form and were measured by means of the minimum-deviation method using a precision spectrometer shown schematically in figure 1 [4]. In the visible and near infrared regions of the spectrum, the index was measured at known emission wavelengths of mercury, cadmium and helium. Beyond 2  $\mu\text{m}$ , a glo-bar was used for the radiant-energy source, and measurements were made at known absorption bands of water, carbon dioxide, polystyrene and 1,2-4 trichlorobenzene. A series of narrow-band interference filters was also used between 3.5 and 10.6  $\mu\text{m}$ . A thermocouple with a cesium iodide window was used for the detector. This instrument has a scale that is accurate to within one second of arc. Therefore, the refractive index of good optical material can be measured within 1 to  $2 \times 10^{-5}$  over a wide wavelength range.

The index was determined for both samples at selected wavelengths from 0.5086  $\mu\text{m}$  to 18.2  $\mu\text{m}$  and at controlled room temperatures near 20°C and 34°C. Each set of experimental data was fitted by a least square solution to a three-term Sellmeier-type dispersion equation [5] of the form

$$n^2 - 1 = \sum_{j=1}^N \frac{A_j \lambda^2}{\lambda^2 - \lambda_j^2}.$$

The index of refraction is represented by  $n$ ,  $\lambda$  is the wavelength of interest in micrometers, the  $\lambda_j$ 's are the calculated wavelengths of maximum absorption and the  $A_j$ 's are the calculated oscillator strengths corresponding to the absorption bands. The  $\lambda_j$ 's and the  $A_j$ 's are not intended to have any

---

1. Figures in brackets indicate the literature references at the end of this paper.

2. The use of company and brand names in this paper is for identification purposes only and in no case does it imply recommendation or endorsement by the National Bureau of Standards, and it does not imply that the materials used in this study are necessarily the best available.

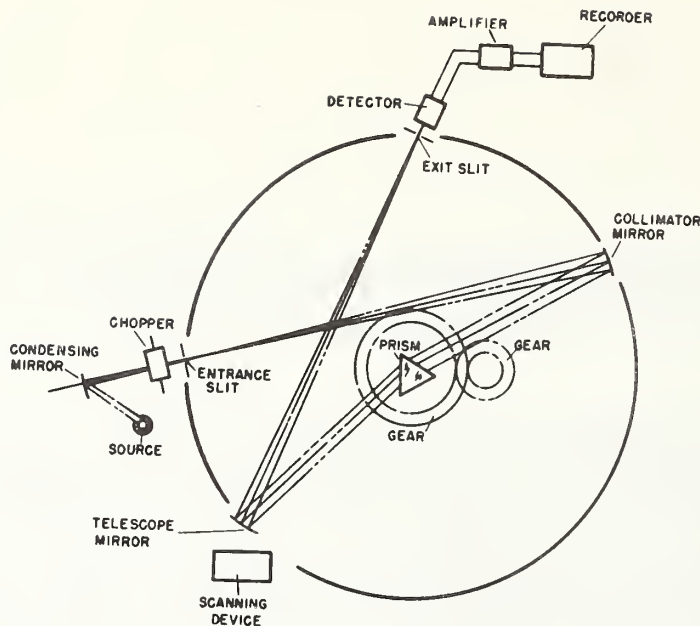


Figure 1. Schematic diagram of the modified Gaertner precision spectrometer showing optical path. The prism is rotated at one-half the rotation rate of the telescope assembly by gear system, thus maintaining the condition of minimum deviation for any wavelength. The scanning device drives the assembly which scans the spectrum to identify lines or bands and determine their approximate scale positions.

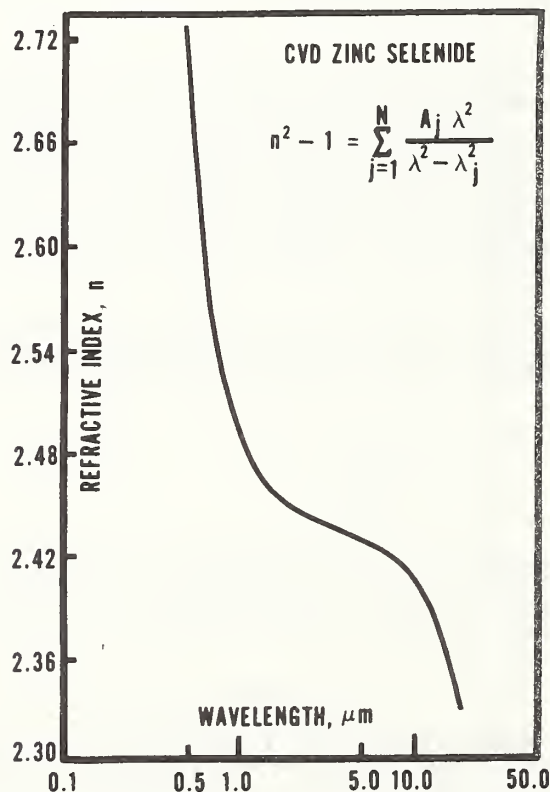


Figure 2. Refractive index of CVD ZnSe (sample B) as a function of wavelength (logarithmic scale). Data at 21°C were calculated from the dispersion equation.

physical significance and are influenced by the wavelength range covered by the experimental data. Primary emphasis is given to procuring a mathematical fit of the measured data useful for interpolation. This equation will fail when an attempt is made to fit data too close to an absorption edge. Because ZnSe is almost totally absorbing below 0.5  $\mu\text{m}$ , it was not possible to fit the data below 0.5461  $\mu\text{m}$  for either sample.

### 2.1.3 Index Data

The constants calculated for each dispersion equation, the specified wavelength range, the number of wavelengths and the overall average absolute residual (the average difference between the experimental values and the calculated values) are given in table 1.

Table 1. Constants of Dispersion Equation for CVD ZnSe

Constant	Sample A		Sample B	
	20.3°C	30.8°C	20.8°C	33.5°C
$A_1$	4.2980149	4.2466487	4.4639521	4.2366336
$A_2$	0.62776557	0.68520488	0.46132463	0.69295365
$A_3$	2.8955633	3.3114671	2.8828867	2.7641692
$\lambda_1$	0.19206300	0.18807700	0.20107634	0.19283319
$\lambda_2$	0.37878260	0.37665162	0.39210520	0.36954401
$\lambda_3$	46.994595	49.694957	47.047590	46.148359
No. of Wavelengths	33	19	38	34
Wavelength Range ( $\mu\text{m}$ )	0.54-18.2	0.54-18.2	0.54-18.2	1.0-18.2
Average Absolute Residual of index $\times 10^{-5}$	6.2	15.6	4.1	7.4

It should be emphasized that these constants refer specifically to these two samples of CVD ZnSe under the stated experimental conditions. The average residual is indicative of the accuracy of the experimental data.

The refractive index was calculated at regular wavelength intervals using each set of fitted parameters. Figure 2 shows the refractive index plotted as a function of wavelength for sample B near 21°C. The index values range from 2.67544 at 0.54  $\mu\text{m}$  to 2.32781 at 18.2  $\mu\text{m}$  and is 2.40278 at 10.6  $\mu\text{m}$ .

In figure 3, the refractive index of sample B is compared with that of sample A and results obtained by other experimenters. The values for sample B are represented by the zero line. All of the data were reduced to a common temperature of 20°C, using the  $dn/dT$  values determined for sample B which will be discussed below. Both single crystals studied by Marple [6] were in the form of prisms and the index was measured at selected wavelengths from the visible to the near IR with a stated accuracy of  $4 \times 10^{-3}$ . From about 1.2 to 2.5  $\mu\text{m}$  the indices of the two samples are about the same, differing from the NBS sample by approximately  $-8$  to  $-4 \times 10^{-5}$ . A prism of Irtran 4, which is hot-pressed polycrystalline ZnSe, was measured by Hilton [7] at selected wavelengths with an estimated uncertainty of  $3 \times 10^{-4}$ . Hilton's data were published in graphical form and the data shown were extracted from the smooth curve. The indices are generally higher than the NBS values by about  $4 \times 10^{-3}$  and agree with the data published on Irtran 4 by Kodak [8] which isn't shown here. The older CVD specimen of ZnSe, sample A, is generally higher than the newer material, sample B, by  $30 \times 10^{-5}$  from the visible to 1  $\mu\text{m}$ , then levels off to within  $\pm 8 \times 10^{-5}$  between 1.6 and 10.8  $\mu\text{m}$ , rising to  $65 \times 10^{-5}$  at 18.2  $\mu\text{m}$ . At 10.6  $\mu\text{m}$ , sample A is higher than B by  $9 \times 10^{-5}$ .

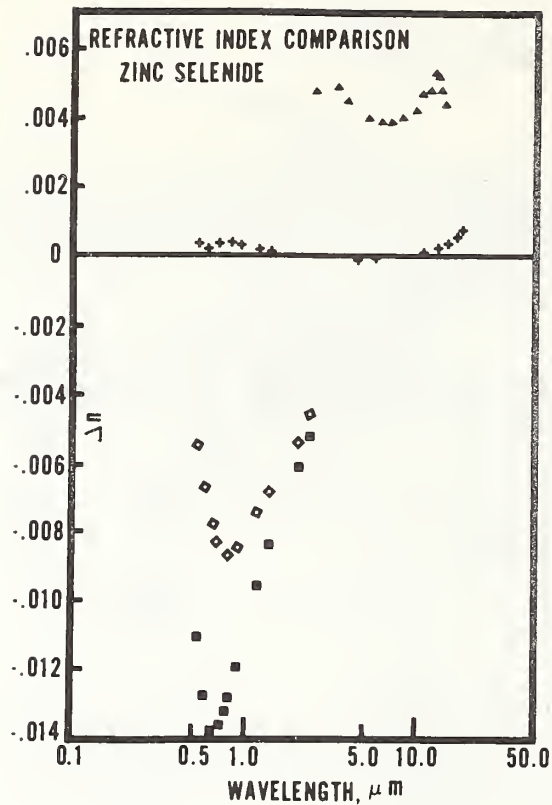


Figure 3. Comparison of NBS index values for CVD ZnSe (sample B) with NBS sample A and values reported by other observers. All data were reduced to 20°C. Refractive index of sample B is represented by the zero line. + NBS sample A, CVD ZnSe; □ Marple, single crystal; ■ Marple single crystal; ▲ Hilton, Irtran 4.

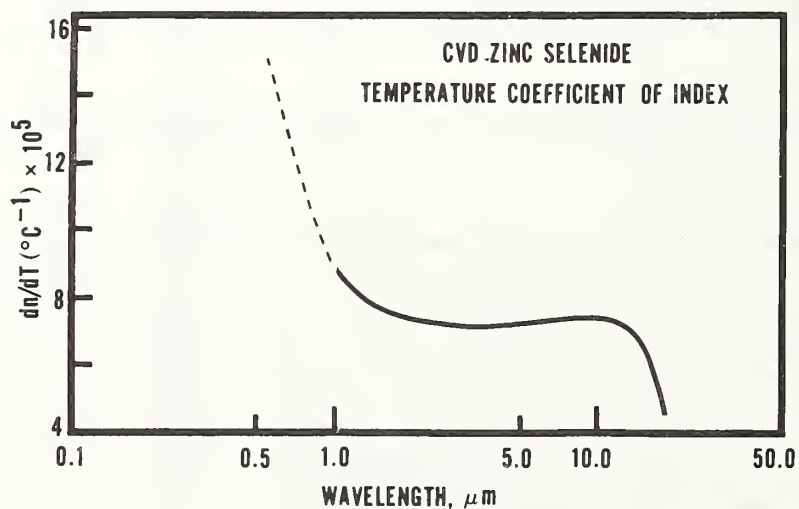


Figure 4. Temperature coefficient of refractive index of CVD ZnSe (sample B) at a mean temperature of 27°C. The solid portion of the curve represents data calculated from index values at two temperatures determined from dispersion equations, and the dashed portion indicates values calculated from raw data.

### 2.1.4 Temperature Coefficient of Index

Sample B was measured at 38 wavelengths at an average room temperature of 33.5°C. An attempt was made to fit the data over the same wavelength range as at 20.8°C, but an acceptable fit could not be obtained. Dropping all wavelengths below 1.0 μm and fitting only the longer IR data, a fit was attained with 34 wavelengths with an average absolute residual of  $7.4 \times 10^{-5}$ . The calculated index values at regular wavelength intervals for both temperatures were used to determine  $dn/dT$  as a function of wavelength from 1.0 to 18.2 μm. This data is shown graphically in figure 4. The solid portion of the curve represents the data calculated from the fitted values and the dashed portion represents values calculated from the raw data. For a mean temperature of 27°C,  $dn/dT$  steadily decreases from about  $15 \times 10^{-5}/^\circ\text{C}$  at 0.5461 μm to a value of  $7.4 \times 10^{-5}/^\circ\text{C}$  at 1.6 μm, remains fairly constant to 12.2 μm, then decreases to  $4.3 \times 10^{-5}/^\circ\text{C}$  at 18.2 μm. These values are considered accurate within  $1.5 \times 10^{-5}$ . However, the change in wavelength of the absorption bands used for wavelength calibration as a result of the increase in temperature is not known. The positive  $dn/dT$  is typical of covalent crystals and is indicative of a shift of the strong absorption edges to longer wavelengths. This could explain the inability to fit the data in the visible region of the spectrum.

The  $dn/dT$  values obtained for the two CVD specimens in this study are compared with those of other researchers [9,10] at 10.6 μm in Table 2.

Table 2. Temperature Coefficient of Refractive Index of CVD Zinc Selenide at 10.6 μm

Reference	Method	Temperature Range (°C)	$dn/dT \times 10^5$
Dodge and Malitson (Sample B)	Minimum-Deviation	20.8-33.5	7.4
(Sample A)	Minimum-Deviation	20.8-30.8	6.8
Feldman, Waxler & Horowitz	Fizeau Interferometry	20-200	6.2
Skolnik & Clark	Laser-Doppler Interferometry	23-62	10.0
Kurdock	Off-Normal Interference	24-69	8.0-9.1

The values range from a low of  $6.2 \times 10^{-5}/^\circ\text{C}$  to a high of  $10.0 \times 10^{-5}/^\circ\text{C}$ . The average of all the values given is  $7.8 \times 10^{-5}/^\circ\text{C}$  which is close to the  $7.4 \times 10^{-5}/^\circ\text{C}$  obtained for sample B and the  $8.0 \times 10^{-5}/^\circ\text{C}$  determined by Kurdock. The same method of measurement was not used in any two laboratories which could account for the discrepancies.

Skolnik and Clark [10] have also determined  $dn/dT$  for Irtran IV and found the value to be  $5.4 \times 10^{-5}/^\circ\text{C}$  at 10.6 μm. This is in fairly good agreement with a value of approximately  $5 \times 10^{-5}/^\circ\text{C}$  determined by Hilton and Jones.

### 2.1.5 Conclusions

The results of this study indicate that the two samples of CVD ZnSe generally agree within 1 to 3  $\times 10^{-4}$  from 0.9 to 15 μm, the spectral region of current interest for use in high-power IR laser systems. The discrepancies in the values of  $dn/dT$  determined by different observers could be due to differences in the material; however, the different methods of measurement should not be ruled out as the cause. These data for the refractive index and  $dn/dT$  are only valid within the stated accuracies for the specimens reported in this study.

### 2.1.6 References

- [1] Sparks, M., J. Appl. Phys. 42, 5029 (1971).
- [2] Feldman, A., I. Malitson, D. Horowitz, R. M. Waxler, and M. Dodge, Laser Induced Damage in Optical Materials: 1974, NBS Special Pub. 414, 141 (1974).
- [3] Tsay, Y., B. Bendow, and S. S. Mitra, Phys. Rev. B 8, 2688 (1972).
- [4] Rodney, William S., and Robert J. Spindler, J. Res. Nat'l. Bur. Stds. (U.S.) 51, 123 (1953).
- [5] Sutton, Loyd E., and Orestes N. Stavroudis, J. Opt. Soc. Am. 51, 901 (1961).
- [6] Marple, D.T.F., J. Appl. Phys. 35, (3), Pt.1 (1964).
- [7] Hilton, A. Ray, and Charlie E. Jones, Appl. Opt. 6, 1513 (1967).
- [8] Kodak Irtran Infrared Optical Materials, Kodak Publication U-72 (1971).
- [9] Feldman, A., I. H. Malitson, D. Horowitz, R. M. Waxler, and M. J. Dodge, Proc. 4th Ann. Conf. on IR Laser Window Materials, ARPA, 117 (1974).
- [10] Skolnik, L.H., and O. M. Clark, Appl. Opt. 13, 1999 (1974).

## 2.2 Photoelastic Constants of Infrared Materials

Albert Feldman, Deane Horowitz and Roy M. Waxler

### 2.2.1 Introduction

Stress can produce inhomogeneous refractive index changes that may be highly deleterious in optical components intended for diffraction limited operation. In high power laser windows, stresses may result from thermal gradients caused by the absorption of intense laser radiation [1]. The stress-optical constants are important parameters needed by laser system designers for calculating the effects of stress on the optical properties of these windows. In this paper we present the methods we employ for measuring stress-optical constants of important infrared window materials. These methods employ null techniques, which have the advantage of being relatively independent of intensity fluctuations in the radiation sources used [2]. Most of the techniques have been discussed previously [3], but are included for completeness. We present data obtained at 10.6  $\mu\text{m}$  on specimens of single crystal Ge, single crystal KCl grown by the reactive atmosphere process (RAP), and single crystal KCl doped with KI. Data are also given for both types of KCl at 0.633  $\mu\text{m}$  and 0.644  $\mu\text{m}$ . Measurements will be continued on these materials so as to improve the precision of the data.

### 2.2.2 The Stress-Optical Constants

The stress-optical effect arises from the dependence on stress,  $\sigma_{kl}$ , of the optical dielectric tensor,  $K_{ij}$ . By convention this relationship is expressed in terms of the change of the reciprocal of the dielectric tensor,  $K_{ij}^{-1}$  (or dielectric impermeability), thus

$$K_{ij}^{-1} = q_{ijkl} \sigma_{kl} \quad (1)$$

where the stress optical constants  $q_{ijkl}$  are the components of a fourth rank tensor and the indices  $ijkl$  each take on values 1, 2, 3. This relationship is frequently expressed in a system of contracted indices (also called the Voigt notation), thus

$$K_m^{-1} = q_{mn} \sigma_n \quad (2)$$

where  $m$  and  $n$  each take on values 1-6. Nye [4] discusses in detail the relationships between the tensors in the full notation and in the contracted notation. For the purposes of this discussion, we use the contracted notation.

In general there exist 36 independent stress-optical constants, but, for our crystals, which are of the cubic class  $m\bar{3}m$ , there are only three independent constants,  $q_{11}$ ,  $q_{12}$  and  $q_{44}$ . To obtain all these coefficients requires three independent measurements of the change of refractive index with stress, but at least one experiment must measure an absolute change of refractive index.

### 2.2.3 Stress-Induced Birefringence

In the present context, stress-induced birefringence is the measure of the relative refractive index change caused by a uniaxial stress. The change is relative because it measures the difference between the changes in refractive index of the two normal polarization modes of radiation propagating through a stressed crystal.

In this experiment, stress is applied along the axis of a specimen in the form of a rectangular prism that has a square cross-section perpendicular to the long axis. The ratio of height to width of a prism is approximately 3:1. For a cubic material two specimens are used with the axis of one specimen along the [100] direction and the axis of the other specimen along the [111] direction. These axes are chosen because the refractive indices are independent of the direction of radiation propagation in the plane perpendicular to the stress axis. The radiation that propagates into the specimen is polarized at 45° with respect to the stress axis. The state of polarization of the emerging radiation, which is determined by the stress-induced birefringence, is analyzed by any of several methods, depending upon the size of the birefringence, and wavelength of the radiation. In the case of Ge, where the stress-optical effect is large and the specimen can support a large stress, one need only to place an analyzer at 90° with respect to the incident polarization angle and photometrically detect nulls or fringes as a function of applied stress. The fringe count,  $N_B$ , per unit applied stress is

$$\frac{dN_B}{d\sigma} = \frac{m}{2} \frac{n^3}{\lambda} \quad \text{qt} \begin{cases} q = q_{11} - q_{12} & \text{for [100] stress} \\ q = q_{44} & \text{for [111] stress} \end{cases} \quad (3)$$

where  $n$  is the zero stress refractive index,  $\lambda$  is the wavelength,  $t$  is the specimen thickness, and  $m$ , which is the number of passes the radiation makes through the specimen, equals one. Increased sensitivity is obtained by allowing multiple passes.

In the case of KCl, it is impossible to obtain a minimum of one fringe, even for multiple passes of the radiation, because the material cannot support large stresses. We therefore employ a birefringence compensator technique for measuring the induced birefringence. For measurements at 10.6  $\mu\text{m}$  we place a specimen of Ge in a stress frame between the KCl specimen and the analyzer. With zero load on the KCl, we stress the Ge to the first null position. After applying a stress to the specimen which removes the null, we adjust the stress of the Ge until the null is restored. Because the Ge has been previously calibrated, we can compute the stress-optical constants of the KCl. For measurements using the above technique in the visible, we employ either a stressed plate of fused silica or a Soleil-Babinet compensator.

Even greater accuracy and precision are possible in the visible if we employ another technique which makes use of a de Senarmont compensator. However, the apparatus for this technique is unavailable for the infrared.

In all cases, multiple passes of the specimen increase the sensitivity of measurement. In figure 5 we show an 8-pass arrangement of the birefringent compensator technique. Multiple passes, however, do not always help if internal strains occur in the specimens. These internal strains can be a major source of error [5].

#### 2.2.4 Absolute Change of Refractive Index

In order to calculate the individual values of  $q_{11}$  and  $q_{12}$ , we require a measurement of the absolute change of the refractive index. For this purpose we use Twyman-Green and/or Fizeau interferometers.

The Twyman-Green interferometer is assembled from components with a laser as the radiation source. The specimen, which must have sufficient optical quality so that fringes are observed at the interferometer output, is mounted in one arm of the interferometer. The shift of fringes as a function of stress is either detected photometrically or viewed on an imaging device. Pyroelectric detectors are used in the infrared at 10.6  $\mu\text{m}$  and photomultipliers are used in the visible and near infrared. Fringes at 10.6  $\mu\text{m}$  are viewed with a thermal image plate or a liquid crystal sheet, while in the visible and near infrared, fringes are viewed with a Si matrix tube and TV-monitor.

The fringe shifts per unit applied [100] stress for stresses parallel and perpendicular to the polarization of the radiation are, respectively,

$$\frac{\Delta N_1}{\Delta \sigma} = \frac{2t}{\lambda} \left[ \frac{n^3}{2} q_{11} - (n-1) s_{12} \right] \quad (4)$$

$$\frac{\Delta N_2}{\Delta \sigma} = \frac{2t}{\lambda} \left[ \frac{n^3}{2} q_{12} - (n-1) s_{12} \right] \quad (5)$$

where  $s_{12}$  is a component of the elastic compliance tensor. If  $s_{12}$  is not known, then it may be determined with Fizeau interferometry. The sample itself functions as a Fizeau interferometer if the faces are polished sufficiently parallel. Fringes are then obtained from the interference between reflections from the front and back surfaces and the shift of these fringes as a function of stress is measured in the same manner as the shift of the Twyman-Green fringes. The fringe shifts per unit applied [100] stress for stresses parallel and perpendicular to the polarization of the radiation are, respectively,

$$\frac{\Delta N_1'}{\Delta \sigma} = \frac{2t}{\lambda} \left[ \frac{n^3}{2} q_{11} - n s_{12} \right] \quad (6)$$

$$\frac{\Delta N_2'}{\Delta \sigma} = \frac{2t}{\lambda} \left[ \frac{n^3}{2} q_{12} - n s_{12} \right] \quad (7)$$

With eqs. (4-7) we can obtain  $q_{11}$ ,  $q_{12}$ , and  $s_{12}$ .

In certain instances, such as in the case of KCl, we are unable to produce a minimum shift of one fringe using standard Twyman-Green or Fizeau interferometers. For this case we have constructed a modified Twyman-Green interferometer that is capable of detecting a 0.01 fringe shift at 10.6  $\mu\text{m}$ . A schematic diagram of the interferometer for use with a CO<sub>2</sub> laser is shown in figure 6. The two arms of the interferometer are in close proximity in order to minimize instabilities due to air currents and vibrations. The effects of vibrations are also minimized by mounting the diagonal mirror onto the same base as the beam splitter and by mounting the two end mirrors on a common base. The specimen arm end mirror, which is mounted on a piezoelectric translator, undergoes a sinusoidal translation thus modulating the output intensity of the interferometer. The reference specimen at 10.6  $\mu\text{m}$  is a crystal of Ge in a compression apparatus. In the visible the reference specimen is fused SiO<sub>2</sub>. We calibrate the reference specimen by measuring the force necessary to produce an integral number fringe shift. Fractional fringes are then obtained by linear interpolation. In operation, the reference specimen is

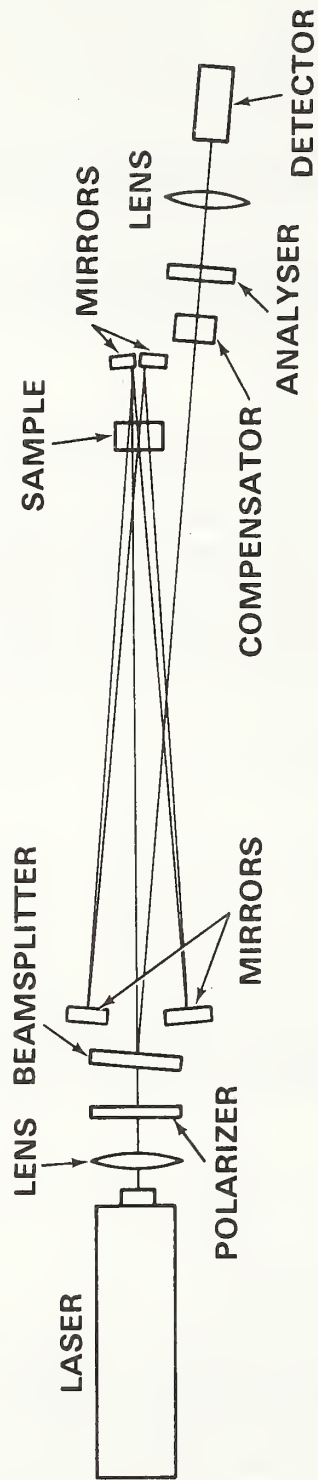


Figure 5. Eight pass measurement of stress birefringence.

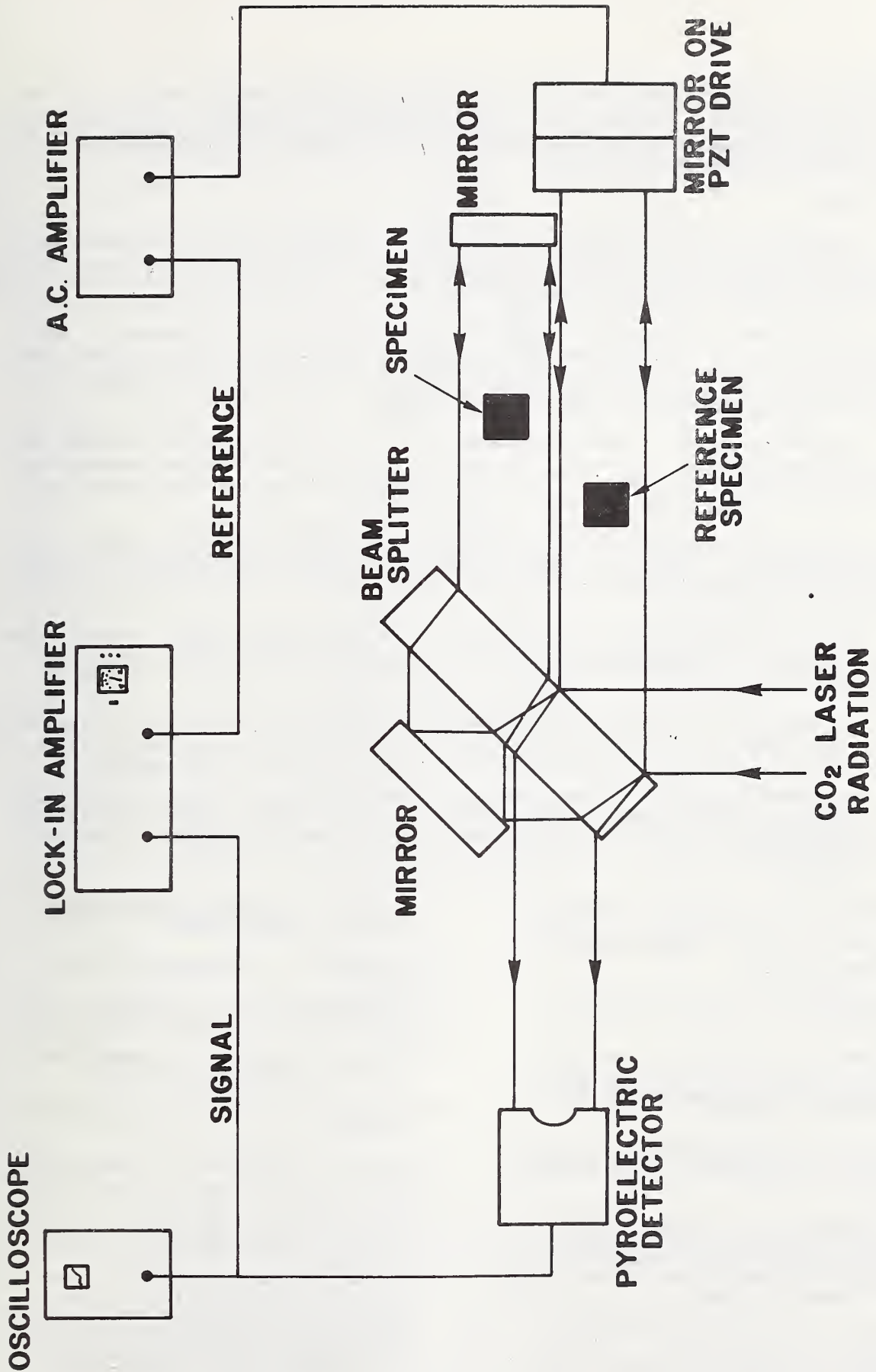


Figure 6. Modified Twyman-Green interferometer for measuring fractional wavelength changes of optic path at 10.6 micrometers.

stressed until the interferometer is at a null, which occurs when the fundamental harmonic of the output intensity is zero. A given stress applied to the unknown specimen will shift the interferometer away from null, whereupon we compensate for this shift by applying an incremental stress to the Ge which brings the interferometer back to null. From these data we then calculate the stress-optical constant using eqs. (4) or (5) provided  $s_{12}$  is known.

## 2.2.5 Results

In Table 3 we show the results we have obtained for Ge compared with earlier reported results [6,7]. We have studied Ge primarily because it is the reference material used in our measurements of the photoelastic constants of other materials in the infrared. Ge is important also as an infrared window material and an infrared acousto-optical material.

Our measurements of the relative stress-optical constants at 10.6  $\mu\text{m}$  are compared with earlier measurements [6] at 2.5  $\mu\text{m}$ . From that earlier work, it can be shown that  $q_{11} - q_{12}$  has a large dispersion, whereas  $q_{44}$  has a small dispersion. This is verified in our results, where the values of  $q_{44}$  at 10.6  $\mu\text{m}$  and 2.5  $\mu\text{m}$  agree to within the experimental error while the value of  $q_{11} - q_{12}$  at 10.6  $\mu\text{m}$  continues the trend of dispersion of shorter wavelength values.

From our measurements of stress-optical constants,  $q_{11}$ ,  $q_{12}$ , and  $q_{44}$ , we have calculated the elasto-optic constants [4]  $p_{11}$ ,  $p_{12}$  and  $p_{44}$  and find a significant difference with the corresponding values obtained by Abrams and Pinnow [7]. Our results indicate that Ge has a smaller figure of merit as an acousto-optic modulator than they calculate from their data.

In Table 4 are presented the values we have obtained for the stress-optical constants of RAP KCl and KCl doped with KI together with earlier reported values [5,8-15]. From our results we cannot infer any difference in the coefficients of these two types of materials. The values for  $q_{11} - q_{12}$  are experimentally determined.

There have been only two reported measurements of the absolute stress-optical constants  $q_{11}$  and  $q_{12}$ , but the values of these respective coefficients in the two reports differ [9,13]. Our results agree most closely with values calculated from the results of Iyengar [9] who actually measured the elasto-optical constants.

Our values for  $q_{11} - q_{12}$  in the visible tend to be slightly higher than earlier reported values. At 10.6  $\mu\text{m}$  we at present cannot attribute any significance to the different values we obtain and the difference of our values from an earlier measurement [14] due to our precision of measurement.

Our values for  $q_{44}$  in the visible appear to fall within the range of earlier reported values. At 10.6  $\mu\text{m}$  our values suggest a small dispersion when compared to the visible. However, this latter result is in disagreement with an earlier measurement [15]. Our larger value suggests a greater distortion problem for KCl.

## 2.2.6 References

- |                                                                                                                                                                                                                                                                                                                                                                                                                                                                                                                                                                                                                                                                                                                                                                                                                                                                                                                                                    |                                                                                                                                                                                                                                                                                                                                                                                                                                                                                                                                                                                                                                                                                                                                                                                                                                                                                                                                                                                            |
|----------------------------------------------------------------------------------------------------------------------------------------------------------------------------------------------------------------------------------------------------------------------------------------------------------------------------------------------------------------------------------------------------------------------------------------------------------------------------------------------------------------------------------------------------------------------------------------------------------------------------------------------------------------------------------------------------------------------------------------------------------------------------------------------------------------------------------------------------------------------------------------------------------------------------------------------------|--------------------------------------------------------------------------------------------------------------------------------------------------------------------------------------------------------------------------------------------------------------------------------------------------------------------------------------------------------------------------------------------------------------------------------------------------------------------------------------------------------------------------------------------------------------------------------------------------------------------------------------------------------------------------------------------------------------------------------------------------------------------------------------------------------------------------------------------------------------------------------------------------------------------------------------------------------------------------------------------|
| <p>[1] Bendow, B., P. D. Gianino, A. Hordvik and L. H. Sholnik, <i>Optics Comm.</i> <b>7</b>, 219 (1973); Bendow, B., and P. D. Gianino, <i>Applied Physics</i> <b>2</b>, 1 (1973).</p> <p>[2] Birnbaum, G., E. Cory and K. Gow, <i>Appl. Optics</i> <b>13</b>, 1660 (1974).</p> <p>[3] Feldman, A., I.H. Malitson, D. Horowitz, R. M. Waxler, and M. Dodge, <i>Laser Induced Damage in Optical Materials:1974</i>, NBS Spec. Publ. 414 (1974).</p> <p>[4] Nye, J. F., <i>Physical Properties of Crystals</i> (Oxford University Press, London 1957) pp. 243-254.</p> <p>[5] Wilkening, W. W., J. Friedman, and C. A. Pitha, "Measurement of Stress-Induced Birefringence in Alkali Halides," Third Conf. on High Power Infrared Laser Window Materials, 1973, AFCEL-TR-74-0085-I.</p> <p>[6] Feldman, A., <i>Phys. Rev.</i> <b>150</b>, 748 (1966).</p> <p>[7] Abrams, R. L., and D. A. Pinnow, <i>J. Appl. Phys.</i> <b>41</b>, 2765 (1970).</p> | <p>[8] Pockels, F., <i>Lehrbuch der Kristalloptik</i>, Leipzig: Teubner (1906).</p> <p>[9] Iyengar, K. S., <i>Nature</i> <b>176</b>, 1119 (1955).</p> <p>[10] Bhagavantam, S., and Y. Krishna Murty, <i>Proc. Indian Acad. Sci. A</i> <b>46</b>, 399 (1957).</p> <p>[11] Bansigir, K. G., and K. S. Iyengar, <i>Proc. Phys. Soc. London</i> <b>71</b> B, 225 (1958).</p> <p>[12] Srinivasan, R., <i>Zeit. f. Physik</i> <b>155</b>, 281-289 (1959).</p> <p>[13] Rao, K. V. Krishna, and V. G. Krishna Murty, <i>Proc. Indian Acad. Sci., Sci.</i> <b>64</b>, 24 (1966).</p> <p>[14] Chen, C. S., J. P. Szczesniak, and J. C. Corelli, <i>J. Appl. Phys.</i> <b>46</b>, 303 (1975).</p> <p>[15] Pitha, C. A., and J. D. Friedman, "Stress-Optical Coefficients of KCl, BaF<sub>2</sub>, CaF<sub>2</sub>, CdTe, TI-1120 and Ti-1173", <i>Proc. of the Fourth Annual Conf. on Infrared Laser Window Materials</i>, Nov. 18-20, 1974. Compiled by C. R. Andrews and C. L. Strecker (1975).</p> |
|----------------------------------------------------------------------------------------------------------------------------------------------------------------------------------------------------------------------------------------------------------------------------------------------------------------------------------------------------------------------------------------------------------------------------------------------------------------------------------------------------------------------------------------------------------------------------------------------------------------------------------------------------------------------------------------------------------------------------------------------------------------------------------------------------------------------------------------------------------------------------------------------------------------------------------------------------|--------------------------------------------------------------------------------------------------------------------------------------------------------------------------------------------------------------------------------------------------------------------------------------------------------------------------------------------------------------------------------------------------------------------------------------------------------------------------------------------------------------------------------------------------------------------------------------------------------------------------------------------------------------------------------------------------------------------------------------------------------------------------------------------------------------------------------------------------------------------------------------------------------------------------------------------------------------------------------------------|

Table 3. Photoelastic Constants of Ge in Units of  $10^{-12} \text{ m}^3/\text{N}$

Coefficients	10.6 $\mu\text{m}$	2.5 $\mu\text{m}$
$q_{11}$	$1.84 \pm .04$	
$q_{12}$	$-.48 \pm .03$	
$q_{11} - q_{12}$	$-.36 \pm .02$	$-.20^a$
$q_{44}$	$1.09 \pm .05$	$-1.12^a$
$p_{11}$	$-.126$	$.27^b$
$p_{12}$	$-.154$	$.235^b$
$p_{44}$	$-.073$	$.125^b$

<sup>a</sup>Ref. [6].

<sup>b</sup>Absolute Values - Ref. [7].

Table 4. Stress-Optical Constants of KCl in Units of  $10^{-12} \text{ m}^2/\text{N}$

$q_{11}$	$q_{12}$	$q_{11} - q_{12}$	$q_{44}$	$\lambda (\mu\text{m})$	Ref.
		1.70	-4.31	0.589	8
4.63	2.92	1.71	-3.62	0.589	9
		1.66	-4.42	0.589	10
		1.47	-4.92	0.589	11
		1.42		0.480	12
5.23	3.58	1.65/1.57	-4.49/-4.74	0.589	13
		1.81		0.633	5
$4.6 \pm .2$	$2.7 \pm .8$	$1.7 \pm .4$	$-3.9 \pm .8$	0.633	This work
		$1.9 \pm .1$	$-4.4 \pm .2$	0.644	This work
$4.6 \pm .2^*$	$2.8 \pm .2^*$	$1.9 \pm .2^*$	$-4.6 \pm .2^*$	0.633	This work
		$1.9 \pm .1^*$	$-4.7 \pm .2^*$	0.644	This work
		2.0	-	10.6	14
			-2.62	10.6	15
		$2.5 \pm 1.0$	$-4.3 \pm .9$	10.6	This work
		$1.5 \pm 0.6^*$	-	10.6	This work

\*Doped with KI.

### 2.3 Revised Photoelastic Data for CVD ZnSe

In Table 5 we list the photoelastic constants obtained at 0.6328  $\mu\text{m}$  and 10.6  $\mu\text{m}$  for CVD ZnSe. Two sets of values are given for 0.6328  $\mu\text{m}$ . The first set [1] was calculated from measurements made on a specimen shortly after it had been stressed beyond the elastic limit. The second set was calculated from measurements on the same specimen 10 months later. The latter set agrees with average values

Table 5. Photoelastic Properties of CVD ZnSe

$\lambda$ ( $\mu\text{m}$ )	0.6328	10.6
$q_{11}$ ( $10^{-12} \text{ m}^2/\text{N}$ )	-1.32 <sup>a</sup> , -1.44 $\pm$ 0.04	-1.46
$q_{12}$ ( $10^{-12} \text{ m}^2/\text{N}$ )	0.28 <sup>a</sup> , 0.17 $\pm$ 0.05	0.51
$q_{11}-q_{12}$ ( $10^{-12} \text{ m}^2/\text{N}$ )	-1.60 <sup>a</sup> , -1.60 $\pm$ 0.01	-1.97
$P_{11}$	-0.10, -0.13	-0.10
$P_{12}$	-0.01, -0.04	0.007

<sup>a</sup>See Ref. 1.

obtained from three other specimens. A comparison of the two sets of data suggests that the absolute photoelastic constants  $q_{11}$  and  $q_{12}$  are altered when the material is stressed beyond the elastic limit, but after an undetermined period of time these constants return to their original values. However, it is interesting to observe that the stress-induced birefringence ( $q_{11}-q_{12}$ ) appears to be unaffected by stressing the material beyond the elastic limit.

The photoelastic data given for 10.6  $\mu\text{m}$  were obtained from birefringence data, modified Twyman-Green data, and elastic constant data obtained at 0.6328  $\mu\text{m}$  (first column Table 6). A calculation of  $dn/dP$  yields  $-3 \times 10^{-12} \text{ m}^2/\text{N}$ , a number which differs significantly from a theoretically calculated value [2]. In fact, there is a sign difference between theory and experiment.

A summary of the elastic moduli we have measured for CVD ZnSe are presented in Table 6. Also shown are the single crystal data of Berlincourt et.al [3]. It is possible to compare the single crystal data to the polycrystalline data by averaging the single crystal moduli. Two different approximations may be made which yield extremal values for the averaged moduli, between which the polycrystalline moduli should fall. The first approximation, due to Voigt [4], who assumes strain continuity in the specimen, yields upper limits to the rigidity modulus  $G$  and bulk modulus  $K$  which we denote by  $G_V$  and  $K_V$ . The second approximation, due to Reuss [5], who assumes stress continuity in the specimen, yields a lower limit to  $G$  and  $K$  which we denote  $G_R$  and  $K_R$ . Values for  $K_V$ ,  $G_V$ ,  $K_R$  and  $G_R$  are listed in Table 6. Our value of  $G$  falls between  $G_V$  and  $G_R$  as predicted by theory [6], but our value of  $K$  is larger than  $K_V$ ,

Table 6. Elastic Properties of ZnSe

	CVD	Single Crystal <sup>a</sup>	Polycrystalline <sup>b</sup>
$s_{11}$ ( $10^{-12} \text{ m}^2/\text{N}$ )	13.9 $\pm$ 0.6	22.6	
$s_{12}$ ( $10^{-12} \text{ m}^2/\text{N}$ )	-4.4 $\pm$ 0.2	-8.49	
$s_{44}$ ( $10^{-12} \text{ m}^2/\text{N}$ )		22.7	
$G$ ( $10^{10} \text{ N/m}^2$ )	2.74 $\pm$ 0.12		2.60 ( $G_R$ ), 3.29 ( $G_V$ )
$K$ ( $10^{10} \text{ N/m}^2$ )	6.6 $\pm$ 0.6		5.95 ( $K_V=K_R$ )

<sup>a</sup>Berlincourt et.al. See Ref. 3.

<sup>b</sup>Calculated from single crystal data. See Ref. 6.

where theory predicts that for cubic crystals  $K_R = K_V$ . Because of the large experimental uncertainty in  $K$ , one must be cautious in drawing conclusions from the latter result. However, Martin [7] suggests that the single crystal data may be in error. He found that of all fifteen ZnS structure semiconductors that he had studied, only the ZnSe and CuCl data deviated significantly from his theory of elastic properties.

In obtaining interferometric data on CVD ZnSe it is imperative that temperature fluctuations be minimized. This is because of the large optic path changes that occur as a function of temperature due to a large positive value of the thermal coefficient of refractive index which adds to the large expansion effect.

### 2.3.1 References

- [1] A. Feldman, I. Malitson, D. Horowitz, R. M. Waxler and M. Dodge, in Laser Induced Damage in Optical Materials:1974, NBS Special Publication 414, Ed. by A. J. Glass and A. H. Guenther (U. S. GPO SD Catalogue No. C13.10:414) p. 141.
- [2] Y. F. Tsay, S. S. Mitra and B. Bendow, Phys. Rev. B 10, 1476 (1974).
- [3] D. Berlincourt, H. Jaffee and L. R. Shiozawa, Phys. Rev. 129, 1009 (1963).
- [4] W. Voigt, Lehrbuch der Kristallphysik, p. 962 (Leipzig: Teubner, 1928).
- [5] A. Reuss, Z. angew. Math. Mech. 9, 55 (1929).
- [6] R. W. Hill, Proc. Phys. Soc. (London). A 65, 349 (1952).
- [7] R. M. Martin, Phys. Rev. B 1, 4005 (1970).

## 2.4 An Improved Stressing Apparatus for Photoelasticity Measurements

Albert Feldman and William J. McKean

Several methods have been employed for measuring the photoelastic constants of solid materials. These use either static [1,2] or dynamic stress [3,4]. In the methods that employ static stress, different types of stressing devices have been employed. In this article we discuss improvements over a previously used stressing frame, which had employed a screw clamp for applying a static load [5]. The apparatus, which is similar to one used by Cuevas and Fritzsche in low temperature piezoresistance measurements [6], incorporates improved features for use at room temperature. The stresses obtained with it are highly uniform over the central portion of the window of a prismatic specimen and thus permit photoelasticity measurements by optical interferometry [7].

Figure 7 shows the stressing apparatus. The main features are the frame, F, the ball bushings, H, the push rod, J, the load cell, M, and the lever arm, C. The frame material is aluminum which provides sufficient strength and is conveniently light. A step at the bottom of the frame allows for solid clamping to a bench plate. The two commercial ball bushings, separated by a spacer, are inserted into the frame with a push fit.

The push rod is made of precision ground steel. The diameter is selected so that when the rod is in place, the ball bushings are slightly preloaded. This eliminates lateral play while allowing virtual friction-free application of stress. The lower end of the push rod contains a conical hole for centering a steel ball several mm in diameter. A member is threaded into the upper end of the push rod to allow for rod length adjustment and thus to take care of sample length variations. A coil spring at the top prevents the push rod from falling by gravity.

The lever arm provides a mechanical advantage of about 8:1. Stress is gradually applied with the lower knurled screw. When the screw is turned, a slight flexing of the lever arm prevents a sudden application of force to the specimen.

A load cell, which is provided with a calibrated digital readout, is attached to the base of the frame with screws. The top of the load cell contains a conical hole for centering another steel ball in line with the hole at the lower end of the push rod.

The specimens are rectangular prisms approximately 1.2 x 1.2 x 3.6 cm. Two opposing rectangular faces of a specimen are ground and polished parallel to act as windows for polarized radiation used in measuring photoelastic constants. The other two rectangular faces are ground parallel to each other and square with the window faces. The ends are ground perpendicular to the other four faces. The specimen is then mounted in metal cups with epoxy adhesive. Masking tape is wrapped around the specimen near the ends to eliminate lateral play when mounting the specimen in the cups. The outer end of each cup contains a conical hole for centering the specimen between the steel balls. The above procedures insure that the stress is transmitted uniformly through the central portion of the specimen.

The apparatus is used as follows: After being mounted in the cups, the specimen with two steel balls at each end is placed between the push rod and the load cell. The upper screw of the lever arm is then rotated to depress the push rod until a slight pressure reading is obtained from the load cell. Stress may now be applied by the knurled lower screw. In our present apparatus forces up to  $10^4$  N have been applied.

This apparatus has several advantages over previously used devices: The ball bushings provide almost friction-free operation without lateral play. The lever arm-push rod arrangement eliminates rotation or twisting inherent in a screw clamp arrangement. The placement of the load cell in line with the specimen permits direct reading of the force applied to the specimen. The method of mounting provides a highly uniform stress in the specimen, with minimum specimen tilt. Thus, stress homogeneity tests indicate that the stress variation across the central 1-cm<sup>2</sup> aperture of the specimen is no more than ±2% of the mean stress value and that the tilt angle of the specimen, measured interferometrically, is less than 2 min. for the maximum applied force.

### 2.4.1 References

- [1] E. G. Coker and L. N. G. Filon, A Treatise on Photo-Elasticity (Cambridge University Press, Cambridge, England, 1957), Chapter III.
- [2] F. Twyman and J. W. Perry, Proc. Phys. Soc. Lond. 34, 151 (1922).
- [3] R. W. Dixon and M. G. Cohen, Appl. Phys. Lett. 8, 205 (1966).
- [4] D. K. Biegelsen, Appl. Phys. Lett. 22, 221 (1973).
- [5] R. M. Waxler and E. N. Farabaugh, J. Res. Natl. Bur. Stand. (U.S.) A 74, 215 (1970).

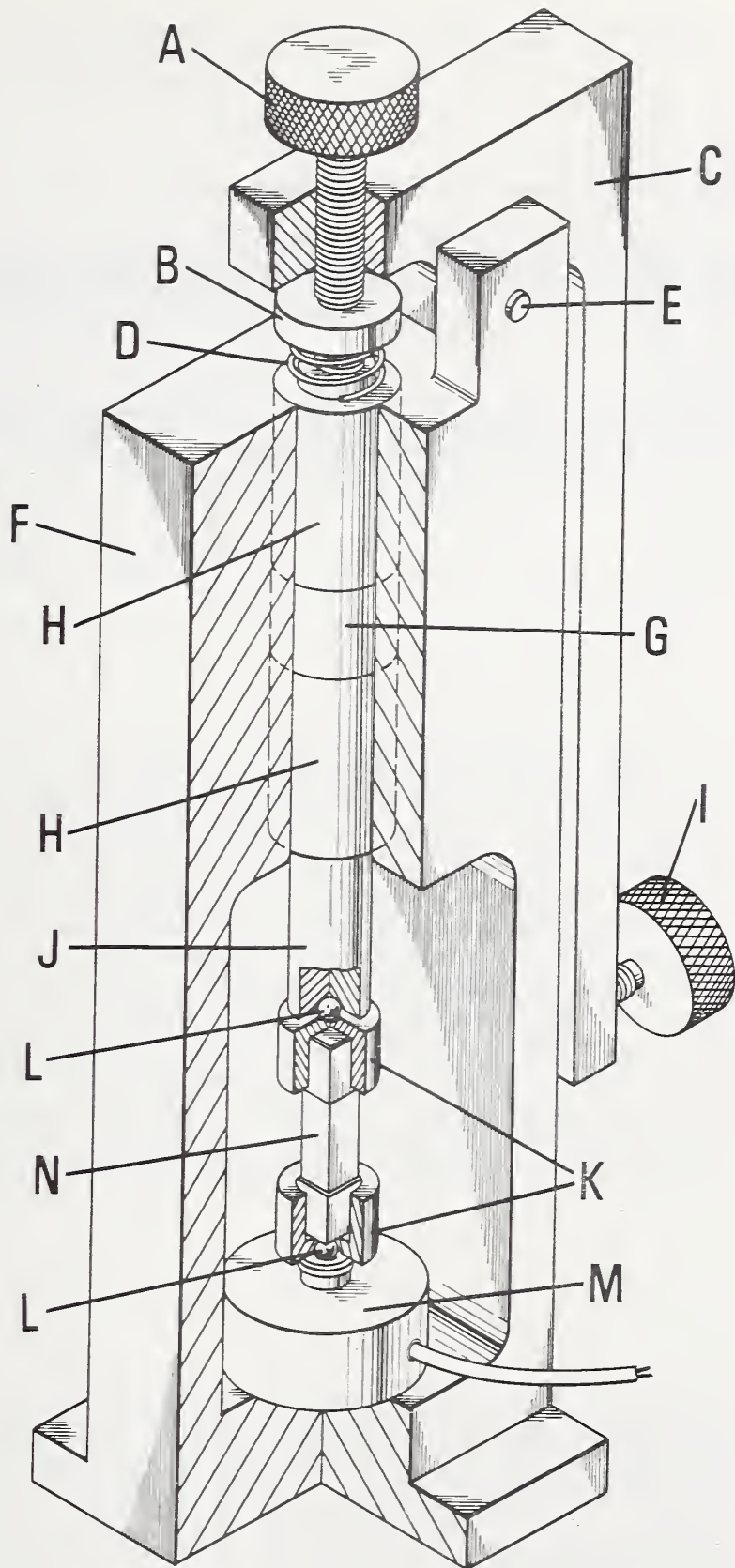


Figure 7. Stressing apparatus. A = adjustment screw with domed tip, B = adjusting member threaded into push rod, C = lever arm, D = coil spring, E = axis, F = frame, G = spacer, H = ball bushing, I = stressing screw with domed tip, J = push rod, K = specimen cup, L = steel ball, M = load cell, N = specimen.

[6] M. Cuevas and H. Fritzsche, Phys. Rev. 137, A1847 (1965).

[7] A. Feldman, I. Malitson, D. Horowitz, R. M. Waxler and M. Dodge, in Laser Induced Damage in Optical Materials: 1974, NBS Special Publication 414, edited by Alexander J. Glass and Arthur H. Guenther (U.S. Government Printing Office, SD Catalogue No. C 13.10:414, 1974), p. 141.

### 3. Acknowledgments

We thank Phillip Klein of the Naval Research Laboratory for supplying the RAP grown KCl, E. Bernal of Honeywell for supplying the KCl doped with KI, and C. Pitha of the Air Force Cambridge Research Laboratory and P. Miles of Raytheon for supplying the CVD ZnSe.

U.S. DEPT. OF COMM. BIBLIOGRAPHIC DATA SHEET		1. PUBLICATION OR REPORT NO. NBSIR-75-781	2. Gov't Accession No.	3. Recipient's Accession No.
4. TITLE AND SUBTITLE  Optical Materials Characterization			5. Publication Date August 1975	
			6. Performing Organization Code	
7. AUTHOR(S) Albert Feldman, Deane Horowitz, Roy M. Waxler, Irving H. Malitson and Marilyn J. Dodge			8. Performing Organ. Report No. NBSIR-75-781	
9. PERFORMING ORGANIZATION NAME AND ADDRESS  NATIONAL BUREAU OF STANDARDS DEPARTMENT OF COMMERCE WASHINGTON, D.C. 20234			10. Project/Task/Work Unit No. 3130442	
			11. Contract/Grant No. 2620	
12. Sponsoring Organization Name and Complete Address (Street, City, State, ZIP)  Advanced Research Projects Agency Arlington, VA 22209			13. Type of Report & Period Covered Semi-Annual Tech. Report 1/1/75 - 7/31/75	
			14. Sponsoring Agency Code	
15. SUPPLEMENTARY NOTES				
16. ABSTRACT (A 200-word or less factual summary of most significant information. If document includes a significant bibliography or literature survey, mention it here.) The refractive index of each of two prismatic samples of chemical vapor deposited (CVD) ZnSe was measured from 0.5086 $\mu\text{m}$ to 18.2 $\mu\text{m}$ by means of the minimum-deviation method on a precision spectrometer. Data were obtained at temperatures near 20 °C and 34 °C and each set of data was fitted to a three-term Sellmeier-type dispersion equation, which permits refractive index interpolation within several parts in $10^{-5}$ . From the data obtained at the two temperatures, $dn/dT$ was calculated for both samples. A comparison of refractive index and $dn/dT$ is made with other types of ZnSe. Preliminary photoelastic data are presented for single crystal specimens of Ge, reactive atmosphere processed (RAP) KCl, and KCl doped with KI. The Ge data, which was obtained at 10.6 $\mu\text{m}$ differ from previously reported data. Data on the two types of KCl were obtained at 10.6 $\mu\text{m}$ , 0.633 $\mu\text{m}$ and 0.644 $\mu\text{m}$ . These data are compared with values from the literature. Also presented are revised photoelasticity data for CVD ZnSe. The design of an improved stressing apparatus that was developed for the measurement of photoelastic constants is discussed.				
17. KEY WORDS (six to twelve entries; alphabetical order; capitalize only the first letter of the first key word unless a proper name; separated by semicolons) Birefringence; elastic constants; infrared-laser window materials; interferometry; KCl; photoelasticity; polycrystalline ZnSe; refractive index; stress-optical constants; thermal coefficient of refractive index; ZnSe.				
18. AVAILABILITY		19. SECURITY CLASS (THIS REPORT)		21. NO. OF PAGES
<input checked="" type="checkbox"/> Unlimited		UNCLASSIFIED		24
<input type="checkbox"/> For Official Distribution. Do Not Release to NTIS		20. SECURITY CLASS (THIS PAGE)		22. Price
<input type="checkbox"/> Order From Sup. of Doc., U.S. Government Printing Office Washington, D.C. 20402, SD Cat. No. C13		UNCLASSIFIED		\$ 3.25
<input checked="" type="checkbox"/> Order From National Technical Information Service (NTIS) Springfield, Virginia 22151				





